| | |
|---|---|
| Title | Electric field control of magnetic domain wall motion via modulation of the Dzyaloshinskii-Moriya interaction |
| Author(s) | Koyama Tomohiro, Nakatani Yoshinobu, Ieda Junichi, Chiba Daichi |
| Citation | Science Advances,4(12),p.eaav0265_1-eaav0265_5 |
| Text Version | Published Journal Article |
| URL | https://jopss.jaea.go.jp/search/servlet/search?5062760 |
| DOI | https://doi.org/10.1126/sciadv.aav0265 |
| Right | © 2018 The Authors, some rights reserved; exclusive licensee American Association for the Advancement of Science. No claim to original U.S. Government Works. Distributed under a Creative Commons Attribution NonCommercial License 4.0 (CC BY-NC). |

PHYSICS

# Electric field control of magnetic domain wall motion via modulation of the Dzyaloshinskii-Moriya interaction

Tomohiro Koyama[1]*, Yoshinobu Nakatani[2], Jun'ichi Ieda[3], Daichi Chiba[1]*



**We show that the electric field (EF) can control the domain wall (DW) velocity in a Pt/Co/Pd asymmetric structure. With the application of a gate voltage, a substantial change in DW velocity up to 50 m/s is observed, which is much greater than that observed in previous studies. Moreover, modulation of a DW velocity exceeding 100 m/s is demonstrated in this study. An EF-induced change in the interfacial Dzyaloshinskii-Moriya interaction (DMI) up to several percent is found to be the origin of the velocity modulation. The DMI-mediated velocity change shown here is a fundamentally different mechanism from that caused by EF-induced anisotropy modulation. Our results will pave the way for the electrical manipulation of spin structures and dynamics via DMI control, which can enhance the performance of spintronic devices.**

## INTRODUCTION

In a ferromagnetic metal (FM)/heavy metal (HM) layered structure, the interfacial Dzyaloshinskii-Moriya interaction (DMI) (iDMI) resulting from structural inversion asymmetry (SIA) and spin-orbit coupling stabilizes a Néel domain wall (DW) with fixed chirality (*1*, *2*) and also a skyrmion (*3*, *4*). The iDMI counters a substantial reduction in DW velocity $v$ because the magnetization precession inside the DW normally caused by the Walker breakdown is suppressed (*5*, *6*). Moreover, the invariance of the chiral DW originating from the iDMI is indispensable for its motion driven by the current-induced spin-orbit torque (*7*–*9*) and ensures the high-speed and robust operation of a race track memory (*10*).

An additional application of an external electric field (EF) to the FM/HM structure represents a method of tuning the SIA and thus can provide a route to efficiently control the DW dynamics via the modulation of the iDMI. A capacitor structure is used to apply an EF to the FM surface through a dielectric layer, and the resultant change in interface magnetism has been reported using various FM thin films (*11*–*22*). However, control of the DW motion caused by an "electrical iDMI gating" has never been achieved. In this study, we demonstrate that an EF application can gate the DW velocity in an iDMI-assisted flow regime. Further experiments clarify that the EF modulation of the iDMI magnitude $D$ rather than the magnetic anisotropy explains the results.

## RESULTS

### Sample preparation and experimental setup

An asymmetric Pt/Co/Pd layered structure capped by a 2-nm-thick MgO layer deposited on a thermally oxidized Si substrate was used for the experiments (see also Materials and Methods). Two samples with different nominal Co thickness $t_{Co}$ (0.78 and 0.98 nm) were prepared. Because of the interfacial magnetic anisotropy at the Pt/Co and Co/Pd interfaces, both samples exhibit perpendicular magnetic anisotropy (PMA). In this structure, a magnetic moment is induced in both the bottom Pt and top Pd layers because of the ferromagnetic proximity effect. The whole part of the Pd layer is expected to be magnetized because its thickness is only 0.4 nm (*19*). Figure 1 shows the schematic image of the device and experimental setup used in this study. The EF was applied to the sample surface through a $HfO_2$ dielectric layer formed by atomic layer deposition (see also Materials and Methods). Here, we defined a positive (negative) gate voltage $V_G$ as corresponding to the direction of the increase (decrease) in the electron density near the sample surface. All experiments shown below were performed at room temperature.

The DW displacement under the application of $V_G$ was observed using a polar magneto-optical Kerr effect (MOKE) microscope. A pulsed perpendicular magnetic field $H_z$ with a duration $\tau$ of 150 ns was applied to nucleate a magnetic domain and drive the DW surrounding it (see also Materials and Methods). The value of $v$ was determined by the following procedure. After making the sample a single-domain state, a domain with an opposite polarity was nucleated by applying a $H_z$ pulse ($|\mu_0 H_z|$ = 210 mT was used to nucleate a domain). Then, a $H_z$ pulse was again applied to expand the nucleated domain. The MOKE images were taken before and after the domain expansion. A typical MOKE image after subtracting two MOKE images is shown in Fig. 1. The dark-colored part corresponds to the region swept by the DW. From the DW displacement ($L$) indicated on the image, $v$ (= $L/\tau$) can be determined.

### DW velocity under application of gate voltage

First, we discuss the $H_z$ dependence of $v$. Figure 2 (A and B) shows the $v - \mu_0 H_z$ characteristics for both samples measured at $V_G$ = 0, +15, and −15 V. By applying high $H_z$, $v$ over 100 m/s is obtained, indicating that the DW motion is in the flow regime (*23*). According to the conventional one-dimensional (1D) model for DW motion, which reasonably describes a free domain expansion in unconfined systems (*24*), $v$ increases linearly with $H_z$ in the flow regime. This behavior was also confirmed experimentally in a symmetric Pt/Co/Pt system (*24*). In contrast, $v$ remains almost saturated for the present asymmetric samples with $t_{Co}$ = 0.78(0.98) nm above $\mu_0 H_z$ ~210(~160) mT. This saturation of $v$ in a high-field regime originated from the iDMI, which has been recently discussed in different asymmetric FM/HM systems (*5*, *6*).

Our results show that the $v - \mu_0 H_z$ curve is modulated by the $V_G$ application. For example, a significant $v$ modulation of up to 50 m/s is achieved around the DW depinning region. Such a large $v$ change has never been reported using the EF effect (*11*–*13*). The EF-induced variation of $v$ for the thermally activated creep regime has been in the

[1]Department of Applied Physics, The University of Tokyo, Bunkyo, Tokyo 113-8656, Japan. [2]University of Electro-Communications, Chofu, Tokyo 182-8585, Japan. [3]Advanced Science Research Center, Japan Atomic Energy Agency, Tokai 319-1195, Japan.
*Corresponding author. Email: tkoyama@ap.t.u-tokyo.ac.jp (T.K.); dchiba@ap.t.u-tokyo.ac.jp (D.C.)

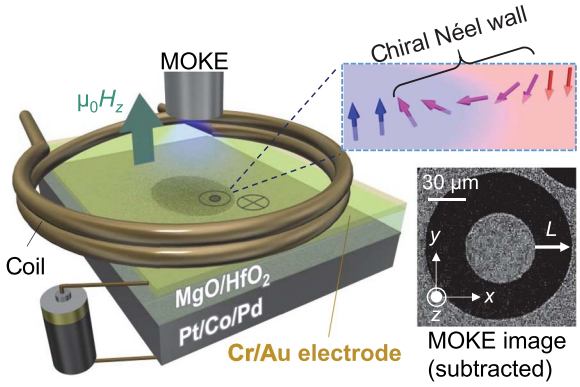


**Fig. 1. Experimental setup.** The capacitor structure consists of the Pt/Co/Pd asymmetric layers, 50-nm $HfO_2$ gate insulator, and Cr/Au electrode. A pulsed perpendicular magnetic field $H_z$ was applied to drive the DW. The $H_z$ was generated using a 500-μm-diameter coil placed on the sample. The DW motion was observed using a MOKE microscope. The typical MOKE image obtained by subtracting two MOKE images taken before and after the application of the pulsed $H_z$ is shown. The DW velocity $v$ was calculated from the DW displacement $L$ by the $H_z$ application.

range from $10^{-3}$ to $10^{-5}$ m/s (*11*–*13*). For the flow regime, only a few meters per second of $v$ change was observed in the Ta/CoFeB/MgO system (*14*). The most important point here is that the saturation $v$ ($v_s$) is changed by the EF application. The insets in Fig. 2 (A and B) show the $v_s$ as a function of $V_G$. The ratios of $v_s$ change between $V_G = \pm 15$ V are 8.2 and 6.7% for the $t_{Co}$ = 0.78 and 0.98 nm samples, respectively.

In the saturation $v$ region, the DW propagates with maintaining its structure as just before the Walker breakdown. It is because in the system with the DMI, the energy dissipation occurs not through the magnetization precession (Walker breakdown) but through the instantaneous nucleation and annihilation of the Bloch lines or small bubbles. Thus, using the Walker breakdown field $H_W$, $v_s$ is expressed as $v_s = \gamma \Delta H_W / \alpha$, where γ is the gyromagnetic ratio, Δ is the DW width, and α is the damping constant. In the large DMI system, $H_W \approx \pi \alpha H_D/2$ (*6*, *7*), where $H_D$ is the DMI effective field. Because $H_D = Dt/(\mu_0 M_s t \Delta)$ (*7*), $v_s$ is finally given by

$$v_s = \frac{\pi}{2} \gamma \frac{Dt}{M_s t} \quad (1)$$

where $t$ is the effective thickness of a ferromagnetic layer, and $Dt$ and $M_s t$ correspond to the areal iDMI magnitude (*25*) and the areal saturation magnetic moment, respectively. $v_s$ for the Pt/Co system with large DMI can be well explained by Eq. 1, as shown in a previous report (*6*). Thus, this model is considered to be applicable to our Pt/Co/Pd structure. $v_s$ is independent of $K_u$, i.e., a change in $K_u$ by the EF does not affect $v_s$ (we have also confirmed this in a 2D case; see section S2). Because the ratio of the $M_s t$ change for both samples is below 1% (see section S1), the EF modulation of $Dt$ is the major factor underlying the $v_s$ change. In the creep regime experiment, the change in the effective PMA is discussed as a possible origin of the creep $v$ modulation (*12*). Thus, the mechanism of the EF modulation of the flow regime $v$ presented here, i.e., $v$ modulation via the DMI change, is largely different from the creep $v$ modulation case. Using Eq. 1, $V_G$ dependence of $Dt$ is quantitatively determined, as shown in Fig. 3 (A and B). The $Dt$ for the sample with $t_{Co}$ = 0.78(0.98) nm is 0.51(0.49) pJ/m at $V_G$ = 0 V, and the modulation ratio between ±15 V is ~8.3(~6.6)%. The modulation ratio of the iDMI in the $t_{Co}$ = 0.78 nm sample is larger than that for the $t_{Co}$ = 0.98 nm

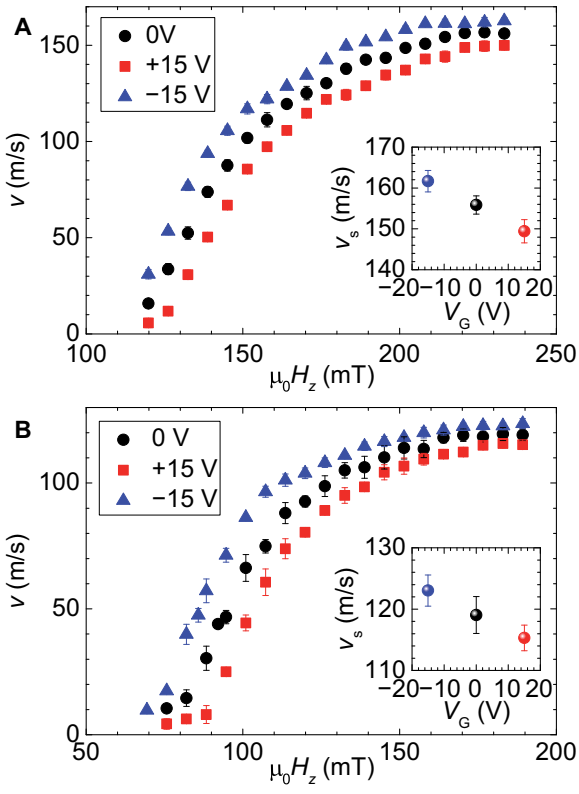


**Fig. 2. Perpendicular magnetic field dependence of DW velocity.** $v$ as a function of $H_z$ obtained under the gate voltage $V_G$ of 0 V (circle), +15 V (square), and −15 V (triangle) for the samples with Co thickness $t_{Co}$ = (**A**) 0.78 nm and (**B**) 0.98 nm is shown. The error bar is the SD of five measurements for each $\mu_0 H_z$. The insets show $V_G$ dependence of the saturation $v$ ($v_s$) in a high $H_z$ regime. The error bar is the SD of $v_s$.

sample, indicating that the EF effect on the iDMI might be more effective in the thinner films. The origin of this may be, for example, the difference in the electron structure of the top Pd caused by the $t_{Co}$-dependent built in strain in the Pd (also see section S1). In this experiment, $V_G$ of ±15 V corresponds to the EF strength applied to the Pd surface of ±0.29 V/nm in consideration of the total thickness of the dielectric layer. Thus, the efficiencies of the $Dt$ modulation by the EF are calculated to be $7.8 \times 10^{-11}$ ($t_{Co}$ = 0.78 nm) and $5.2 \times 10^{-11}$ (0.98 nm) pJ/V, respectively. These values are close to the previous study using the Au/Fe/MgO system (*18*).

## Gate voltage effect on the DMI effective field

To investigate the EF effect on the iDMI more directly, the magnitude of $H_D$, which acts on the local magnetizations inside the DW, was determined from the $H_z$-driven DW motion under additional static in-plane magnetic fields (*5*, *6*, *23*). Figure 4A shows the static $x$-field $H_x$ dependence of $v$ obtained at $|\mu_0 H_z|$ = 178 mT for the sample with $t_{Co}$ = 0.98 nm under $V_G$ = 0 V. Two different situations where the negatively polarized (N domain) and positively polarized (P domain) domain expands were investigated. As shown in the subtracted MOKE image in Fig. 4A, the DW displacement along the $x$ axis is asymmetric when $H_x$ is applied. $v$ increases with the positive $\mu_0 H_x$ when the N domain expands. The opposite $\mu_0 H_x$ dependence is observed in the case of the P domain expansion. The asymmetric $\mu_0 H_x$ dependence of $v$ manifests that the magnetization inside the DW

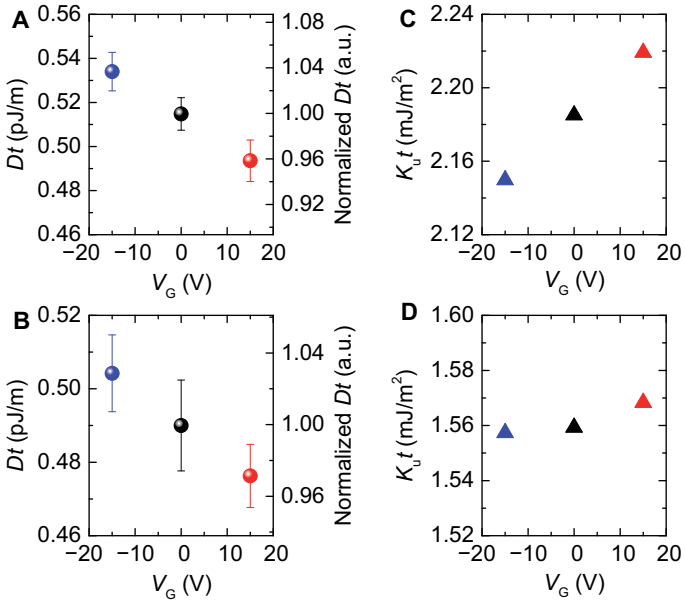


**Fig. 3. Gate voltage dependence of the areal iDMI and PMA.** $V_G$ dependence of the areal iDMI magnitude $Dt$ for the sample with $t_{Co}$ = (**A**) 0.78 nm and (**B**) 0.98 nm is shown. $Dt$ is determined using the $v_s$ and areal magnetic moment of the sample following Eq. 1. a.u., arbitrary units. The error bar indicates the error of $v_s$. Areal PMA energy $K_u t$ as a function of $V_G$ for the $t_{Co}$ = (**C**) 0.78 nm and (**D**) 0.98 nm samples is shown.

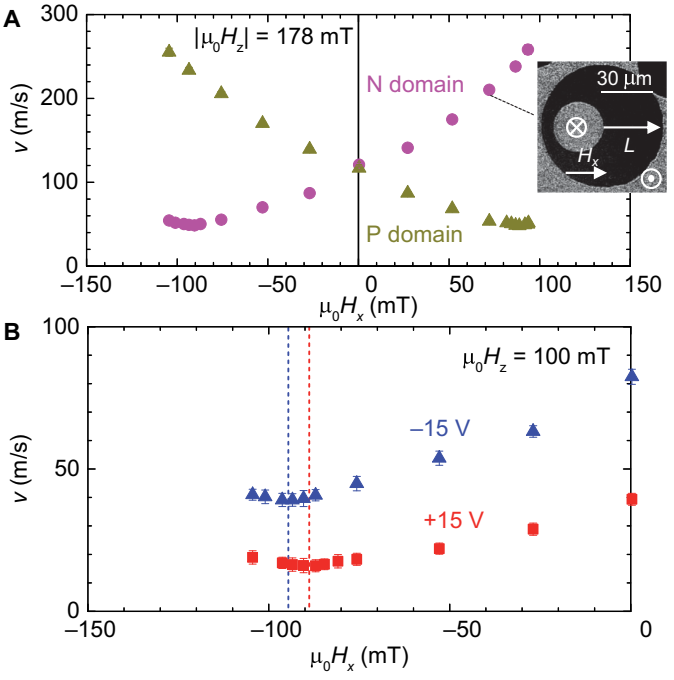


**Fig. 4. In-plane field dependence of the DW velocity under gate voltage.** (**A**) $v$ as a function of static in-plane magnetic field $H_x$ for the sample with 0.98-nm Co thickness. The negatively polarized (N domain) and positively polarized (P domain) domain expansion cases are displayed. $\mu_0 H_z$ of 178 mT was applied to drive the DW. The MOKE image is the subtracted image obtained under $\mu_0 H_x$ = +72 mT for N domain case. (**B**) $v$ measured under an in-plane static field $H_x$ at $V_G$ = +15 V (circle) and −15 V (triangle) for the sample with $t_{Co}$ = 0.98 nm. $|\mu_0 H_z|$ of 100 mT was applied to drive the DW. The dashed lines indicate the DMI effective fields $H_D$ for $V_G$ = +15 and −15 V. The error bar is the SD of 10 measurements for each $\mu_0 H_x$.

surrounding the N (P) domain directs outward (inward) normal to the DW plane, i.e., the left-handed chiral Néel DW is formed in our Pt/Co/Pd systems. The type of DW chirality in the present Pt/Co/Pd system is consistent with that for the Pt/Co systems (*2*, *26*). Next, $V_G$ application effect is checked. Here, the situation in which the N domain expanded by $H_z$ is focused. In the experiments shown in Fig. 4B, DW motion was induced by a $|\mu_0 H_z|$ of 100 mT under the application of $H_x$. In both $V_G$ cases (+15 and −15 V), $v$ decreased with negative $H_x$ because of the DW chirality. For this sample, the $v$ minimum in the $v - \mu_0 H_x$ characteristics appears at approximately $\mu_0 H_x$ = −88(−95) mT ($\equiv \mu_0 H_x^{min}$) for $V_G$ = +15 (−15) V, where $|H_x^{min}|$ corresponds to the $H_D$ of this sample (*6*, *23*). The position of $H_x^{min}$ depends on $V_G$, i.e., $H_D$ is modulated by the application of $V_G$. The ratio of the change in $H_x^{min}$ between $V_G$ = ±15 V is ~8%.

Within the framework of the 1D analytical model, $H_D$ is also proportional to $Dt$ as follows (*7*)

$$H_D = \frac{Dt}{M_s t \Delta} \quad (2)$$

where $\Delta$ (= $\sqrt{A/K_u}$) is the DW width parameter ($K_u$ and $A$ are the PMA energy density and exchange stiffness, respectively). Thus, the changes in $K_u$ and $A$ can represent another factor for the EF-induced $H_D$ change. Figure 3 (C and D) shows the $V_G$ dependences of $K_u t$ for $t_{Co}$ = 0.78 and 0.98 nm samples, respectively. $K_u t$ increases with positive $V_G$ in both samples, and the difference in $K_u t$ between $V_G$ = ±15 V for the sample with $t_{Co}$ = 0.98 nm is 0.7%, as shown in Fig. 3D (see section S1). In this case, the $A$ change must be ~17% if the EF-induced change in $H_D$ obtained here was only caused by the modulation of $\Delta$. However, the EF-induced change in $A$ (or the exchange coupling) is expected to be a few percent at most (*20*, *21*). Thus, the EF change in $H_D$ was most likely caused by the $V_G$ modulation of $Dt$. From the experimental $H_D$ value, the $Dt$ determined from Eq. 2 was 0.32(0.35) pJ/m for $V_G$ = +15(−15) V by assuming a constant $A = 1.6 \times 10^{-11}$ J/m (*6*, *7*). The magnitudes of $Dt$ determined from $v_s$ and $H_D$ measurements are consistent within a factor of ~1.5. The assumption of $A$ may provide one reason for this slight difference.

## DISCUSSION

The iDMI of the present sample is mainly dominated by the Pt/Co and Co/Pd interfaces. Because of the screening effect, the EF is almost shielded in the top Pd layer, i.e., the EF is hindered from reaching the deeper metallic layers (Co and Pt). Thus, the EF effect on the electronic structure (*27*) in the Pd layer plays a major role in the modulation of the iDMI (particularly the iDMI only at the Co/Pd interface). It is known that the iDMI in the FM/HM layered structure is attributed to the *d*-electron states at the Fermi level of the HM (*28*). Thus, in this experiment, the modulation of the outermost 4*d* electron state in the Pd is considered to be caused by the EF application, resulting in the change in the iDMI at the Co/Pd interface. The EF application also results in a change in the Co/Pd interfacial PMA energy. Although the iDMI is expected to positively correlate with the PMA if they originated at the same interface (*9*), the opposite EF response between $Dt$ and $K_u$ was observed in the present experiment (see Fig. 3). One possible explanation for this contradiction is as follows: the $Dt$ ($K_u t$) in the

present sample is the sum of the iDMIs (interfacial PMAs) at the Co/Pd and Pt/Co interfaces

$$Dt = |D^{\mathrm{Pt}}t| - |D^{\mathrm{Pd}}t|$$
$$K_{\mathrm{u}}t = K_{\mathrm{u}}{}^{\mathrm{Pt}}t + K_{\mathrm{u}}{}^{\mathrm{Pd}}t \quad (3)$$

where $D^{\mathrm{Pt(Pd)}}t$ [$K_{\mathrm{u}}{}^{\mathrm{Pt(Pd)}}t$] is the areal iDMI (areal PMA energy) at the Pt/Co (Co/Pd) interface. Note that the negative sign before the $|D^{\mathrm{Pd}}t|$ term is due to the inverted stacking of Pt/Co and Co/Pd. Equation 3 shows that the EF-induced increase in $|D^{\mathrm{Pd}}t|$ results in a decrease in the total iDMI ($Dt$) of the entire system because $|D^{\mathrm{Pt}}t|$, which is the iDMI at the deeper interface, should be unchanged because of the screening effect. On the other hand, the increase in $K_{\mathrm{u}}{}^{\mathrm{Pd}}t$ simply results in the enhancement of total PMA energy ($K_{\mathrm{u}}t$). This may represent a scenario for understanding the opposite response of $Dt$ and $K_{\mathrm{u}}t$ to the EF. In addition to the above interpretation, the change in iDMI and PMA may have originated at the Pd/MgO interface instead of the Co/Pd interface. In this case, the EF-induced change in the interfacial Rashba effect (*29*, *30*) may be important for understanding the result.

In summary, we demonstrate the gating control of DW motion using Pt/Co/Pd asymmetric systems. The iDMI-stabilized $v$ and $H_{\mathrm{D}}$ are modulated by the EF application. The change in $v$ via the modulation of the DMI has a fundamentally different origin compared with the PMA-mediated case as reported in the Ta/CoFeB/MgO system (*14*). The electrical manipulation of the DMI demonstrated here is expected to provide a novel function for future spintronic devices based on chiral DWs or skyrmions.

## MATERIALS AND METHODS

### Film deposition and device fabrication

Layers composed of Ta(2.6 nm)/Pt(2.4)/Co($t_{\mathrm{Co}}$)/Pd(0.4)/MgO(2.0) were deposited on a thermally oxidized Si substrate using radio frequency sputtering. The base pressure of the sputter chamber was below $1.0 \times 10^{-6}$ Pa, and Xe process gas was used for the deposition. The x-ray diffraction profile indicated that the Pt layer has a face-centered cubic (111) texture. To fabricate the capacitor structure, a 50-nm $HfO_2$ gate dielectric layer was deposited on the film at 150°C in an atomic layer deposition chamber. Subsequently, a Cr(2)/Au(10) gate electrode with a size of 300 × 300 μm was formed by a lift-off process. The magnitude of the leakage current under the application of $V_{\mathrm{G}} = \pm 15$ V was below 500 pA. Note that the Pd layer on the Co layer acts to suppress unwanted domain nucleation; in the sample without the Pd layer, the distances between nucleated domains were too short to measure the DW velocity under the high-field regime.

### Pulsed field application

$H_z$ was generated using a small coil with a diameter of 500 μm placed on the device (see Fig. 1). To generate $H_z$, a pulsed current supplied from a customized high-voltage pulse generator was injected into the small coil. A rectangular-shaped pulse was confirmed by monitoring the voltage across the resistor connected with the coil in series.

## SUPPLEMENTARY MATERIALS

Supplementary material for this article is available at http://advances.sciencemag.org/cgi/content/full/4/12/eaav0265/DC1

Section S1. EF effect on areal magnetic moment and anisotropy energy

Section S2. Numerical calculation of the saturation DW velocity

Fig. S1. Schematic illustration of the capacitor structure for the areal magnetization measurement.

Fig. S2. In-plane magnetization curves for the studied samples.

Fig. S3. Simulated DW velocities as a function of external magnetic field and the anisotropy and DMI dependences of the DW velocity.

Table S1. Summary of the capacitances for the capacitors.

Reference (*31*)

## REFERENCES AND NOTES


1. G. Chen, T. Ma, A. T. N'Diaye, H. Kwon, C. Won, Y. Wu, A. K. Schmid, Tailoring the chirality of magnetic domain walls by interface engineering. *Nat. Commun.* **4**, 2671 (2013).
2. J.-P. Tetienne, T. Hingant, L. J. Martínez, S. Rohart, A. Thiaville, L. Diez, K. Garcia, J.-P. Adam, J.-V. Kim, J.-F. Roch, I. M. Miron, G. Gaudin, L. Vila, B. Ocker, D. Ravelosona, V. Jacques, The nature of domain walls in ultrathin ferromagnets revealed by scanning nanomagnetometry. *Nat. Commun.* **6**, 6733 (2015).
3. A. Fert, V. Cros, J. Sampaio, Skyrmions on the track. *Nat. Nanotechnol.* **8**, 152–156 (2013).
4. W. Jiang, G. Chen, K. Liu, J. Zang, S. G. E. te Velthuis, A. Hoffman, Skyrmions in magnetic multilayers. *Phys. Rep.* **704**, 1–49 (2017).
5. Y. Yoshimura, K.-J. Kim, T. Taniguchi, T. Tono, K. Ueda, R. Hiramatsu, T. Moriyama, K. Yamada, Y. Nakatani, T. Ono, Soliton-like magnetic domain wall motion induced by the interfacial Dzyaloshinskii-Moriya interaction. *Nat. Phys.* **12**, 157–161 (2016).
6. T. H. Pham, J. Vogel, J. Sampaio, M. Vaňatka, J.-C. Rojas-Sánchez, M. Bonfim, D. S. Chaves, F. Choueikani, P. Ohresser, E. Otero, A. Thiaville, S. Pizzini, Very large domain wall velocities in Pt/Co/Gd trilayers with Dzyaloshinskii-Moriya interaction. *Europhys. Lett.* **113**, 67001 (2016).
7. A. Thiaville, S. Rohart, É. Jué, V. Cros, A. Fert, Dynamics of Dzyaloshinskii domain walls in ultrathin magnetic films. *Europhys. Lett.* **100**, 57002 (2012).
8. S. Emori, U. Bauer, S.-M. Ahn, E. Martinez, G. S. D. Beach, Current-driven dynamics of chiral ferromagnetic domain walls. *Nat. Mater.* **12**, 611–616 (2013).
9. K.-S. Ryu, L. Thomas, S.-H. Yang, S. Parkin, Chiral spin torque at magnetic domain walls. *Nat. Nanotechnol.* **8**, 527–533 (2013).
10. S. S. P. Parkin, M. Hayashi, L. Thomas, Magnetic domain-wall racetrack memory. *Science* **320**, 190–194 (2008).
11. A. J. Schellekens, A. van den Brink, J. H. Franken, H. J. M. Swagten, B. Koopmans, Electric-field control of domain wall motion in perpendicularly magnetized materials. *Nat. Commun.* **3**, 847 (2012).
12. D. Chiba, M. Kawaguchi, S. Fukami, N. Ishiwata, K. Shimamura, K. Kobayashi, T. Ono, Electric-field control of magnetic domain-wall velocity in ultrathin cobalt with perpendicular magnetization. *Nat. Commun.* **3**, 888 (2012).
13. A. Bernand-Mantel, L. Herrera-Diez, L. Ranno, S. Pizzini, J. Vogel, D. Givord, S. Auffret, O. Boulle, I. M. Miron, G. Gaudin, Electric-field control of domain wall nucleation and pinning in a metallic ferromagnet. *Appl. Phys. Lett.* **102**, 122406 (2013).
14. W. Lin, N. Vernier, G. Agnus, K. Garcia, B. Ocker, W. Zhao, E. E. Fullerton, D. Ravelosona, Universal domain wall dynamics under electric field in Ta/CoFeB/MgO devices with perpendicular anisotropy. *Nat. Commun.* **7**, 13532 (2016).
15. M. Weisheit, S. Fähler, A. Marty, Y. Souche, C. Poinsignon, D. Givord, Electric field-induced modification of magnetism in thin-film ferromagnets. *Science* **315**, 349–351 (2007).
16. T. Maruyama, Y. Shiota, T. Nozaki, K. Ohta, N. Toda, M. Mizuguchi, A. A. Tulapurkar, T. Shinjo, M. Shiraishi, S. Mizukami, Y. Ando, Y. Suzuki, Large voltage-induced magnetic anisotropy change in a few atomic layers of iron. *Nat. Nanotechnol.* **4**, 158–161 (2009).
17. D. Chiba, S. Fukami, K. Shimamura, N. Ishiwata, K. Kobayashi, T. Ono, Electrical control of the ferromagnetic phase transition in cobalt at room temperature. *Nat. Mater.* **10**, 853–856 (2011).
18. K. Nawaoka, S. Miwa, Y. Shiota, N. Mizuochi, Y. Suzuki, Voltage induction of interfacial Dzyaloshinskii–Moriya interaction in Au/Fe/MgO artificial multilayer. *Appl. Phys. Express* **8**, 063004 (2015).
19. Y. Hibino, T. Koyama, A. Obinata, K. Miwa, S. Ono, D. Chiba, Electric field modulation of magnetic anisotropy in perpendicularly magnetized Pt/Co structure with a Pd top layer. *Appl. Phys. Express* **8**, 113002 (2015).
20. T. Dohi, S. Kanai, A. Okada, F. Matsukura, H. Ohno, Effect of electric-field modulation of magnetic parameters on domain structure in MgO/CoFeB. *AIP Adv.* **6**, 075017 (2016).
21. F. Ando, K. T. Yamada, T. Koyama, M. Ishibashi, Y. Shiota, T. Moriyama, D. Chiba, T. Ono, Microscopic origin of electric-field-induced modulation of Curie temperature in cobalt. *Appl. Phys. Express* **11**, 073002 (2018).

22. T. Srivastava, M. Schott, R. Juge, V. Křižáková, M. Belmeguenai, Y. Roussigné, A. Bernand-Mantel, L. Ranno, S. Pizzini, S.-M. Chérif, A. Stashkevich, S. Auffret, O. Boulle, G. Gaudin, M. Chshiev, C. Baraduc, H. Béa, Large-voltage tuning of Dzyaloshinskii–Moriya interactions: A route toward dynamic control of skyrmion chirality. *Nano Lett.* **18**, 4871–4877 (2018).
23. M. Vaňatka, J.-C. Sánchez, J. Vogel, M. Bonfim, M. Belmeguenai, Y. Roussigné, A. Stashkevich, A. Thiaville, S. Pizzini, Velocity asymmetry of Dzyaloshinskii domain walls in the creep and flow regimes. *J. Phys. Condens. Matter* **27**, 326002 (2015).
24. P. J. Metaxas, J. P. Jamet, A. Mougin, M. Cormier, J. Ferré, V. Baltz, B. Rodmacq, B. Dieny, R. L. Stamps, Creep and Flow Regimes of magnetic domain-wall motion in ultrathin Pt/Co/Pt films with perpendicular anisotropy. *Phys. Rev. Lett.* **99**, 217208 (2007).
25. M. Belmeguenai, J.-P. Adam, Y. Roussigné, S. Eimer, T. Devolder, J.-V. Kim, S. M. Cherif, A. Stashkevich, A. Thiaville, Interfacial Dzyaloshinskii-Moriya interaction in perpendicularly magnetized Pt/Co/$AlO_x$ ultrathin films measured by Brillouin light spectroscopy. *Phys. Rev. B* **91**, 180405 (2015).
26. S. Pizzini, J. Vogel, S. Rohart, L. D. Buda-Prejbeanu, E. Jué, O. Boulle, I. M. Miron, C. K. Safeer, S. Auffret, G. Gaudin, A. Thiaville, Chirality-induced asymmetric magnetic nucleation in Pt/Co/$AlO_x$ ultrathin microstructures. *Phys. Rev. Lett.* **113**, 047203 (2014).
27. K. Nakamura, R. Shimabukuro, Y. Fujiwara, T. Akiyama, T. Ito, A. J. Freeman, Giant modification of the magnetocrystalline anisotropy in transition-metal monolayers by an external electric field. *Phys. Rev. Lett.* **102**, 187201 (2009).
28. H. Yang, A. Thiaville, S. Rohart, A. Fert, M. Chshiev, Anatomy of Dzyaloshinskii-Moriya interaction at Co/Pt interfaces. *Phys. Rev. Lett.* **115**, 267210 (2015).
29. A. Kundu, S. Zhang, Dzyaloshinskii-Moriya interaction mediated by spin-polarized band with Rashba spin-orbit coupling. *Phys. Rev. B* **92**, 094434 (2015).
30. S. E. Barnes, J. Ieda, S. Maekawa, Rashba spin-orbit anisotropy and the electric field control of magnetism. *Sci. Rep.* **4**, 4105 (2014).
31. Y.-C. Lau, P. Sheng, S. Mitani, D. Chiba, M. Hayashi, Electric field modulation of the non-linear areal magnetic anisotropy energy. *Appl. Phys. Lett.* **110**, 022405 (2017).

**Acknowledgments**
**Funding:** This work was partly supported by JSPS KAKENHI grant numbers JP15H05419, JP25220604, and JP16K05424; the Spintronics Research Network of Japan; and the Collaborative Research Program of Institute for Chemical Research, Kyoto University (#2018-63). **Author contributions:** T.K. and D.C. planned the study. T.K. fabricated the device and corrected and analyzed the data. Y.N. performed the simulation. J.I. conducted the theoretical development. T.K. wrote the manuscript with input from J.I. and D.C. All authors discussed the results. **Competing interests:** The authors declare that they have no competing interests. **Data and materials availability:** All data needed to evaluate the conclusions in the paper are present in the paper and/or the Supplementary Materials. Additional data related to this paper may be requested from the authors.

Submitted 7 August 2018
Accepted 20 November 2018
Published 21 December 2018
10.1126/sciadv.aav0265

**Citation:** T. Koyama, Y. Nakatani, J. Ieda, D. Chiba, Electric field control of magnetic domain wall motion via modulation of the Dzyaloshinskii-Moriya interaction. *Sci. Adv.* **4**, eaav0265 (2018).

ScienceAdvances

# Electric field control of magnetic domain wall motion via modulation of the Dzyaloshinskii-Moriya interaction

Tomohiro Koyama, Yoshinobu Nakatani, Jun'ichi Ieda and Daichi Chiba

*Sci Adv* **4** (12), eaav0265.
DOI: 10.1126/sciadv.aav0265